Biochemical studies on a SNP and Patient Mutations in Mitochondrial B_{12} Proteins

A thesis submitted by

Harsha Gouda

In partial fulfillment of degree of

BS-MS Dual degree at

Department of Chemistry

Indian Institute of Science Education and Research, Pune

May 2018

B

Certificate

This is to certify that this dissertation entitled "**Biochemical studies on a SNP and Patient Mutations in Mitochondrial B_{12} Proteins**" towards the partial fulfilment of the BS-MS dual degree program at the Indian Institute of Science Education and Research, Pune represents study/work carried out by "**Harsha Gouda**" at "**Department of Biological Chemistry, University of Michigan, Ann Arbor**" under the supervision of "**Prof. Ruma Banerjee, Vincent Massey Collegiate Professor, Department of Biological Chemistry**" during the academic year 2018-2019

Signature of student

Date: May 27, 2019

Signature of supervisor

Date: May 27, 2019

IISER PUNE

Declaration

I hereby declare that the matter embodied in the report entitled "**Biochemical studies on a SNP and Patient Mutations in Mitochondrial B_{12} Proteins**" is the result of work carried out by me at the "**Department of Biological Chemistry, University of Michigan, Ann Arbor**", under the supervision of "**Prof. Ruma Banerjee**" and the same has not been submitted elsewhere for any other degree.

Signature of student

Date: May 27, 2019

Signature of supervisor

Date: May 27, 2019

Acknowledgements:

The completion of this study would have been not possible without the support form a lot of people. I would like to take this opportunity to thank everyone that helped me complete the study.

At first, I would like to thank my supervisor Prof. Ruma Banerjee for providing me the opportunity to be a part of her lab and her valuable intellectual, financial and moral support throughout the study, her expertise and input have made the study possible. I would like to thank Drs. Gregory Campanello and Markus Rutez for their exceptional mentorship in training me in various biochemical assays and shaping me to be a better researcher. I would also like to express my gratitude to Dr. Romila Mascarenhas for helping me set up crystallization trays of mutant proteins and Dr.Zhu Li for her valuable input and support. My sincere appreciation to all other current and past members of Prof. Banerjee's lab with whom I interacted during my stay in particular, Drs. Victor Vitvitsky, Aaron Landry, Teresa Vitale, Roshan Kumar and Sojin Moon for their valuable advice and help with lab techniques. Thanks also to graduate and undergraduate students Aditi Gupta, Albert Kallon, Trever Bostelaar, and Liam McDevitt for providing an amusing workspace environment. I would also like to take this opportunity to thank my thesis advisor Dr. Amrita Hazra, for her valuable input to the study. I am thankful to the IISER-Michigan science exchange program for providing me this wonderful opportunity to be a part of this program.

Finally, I would like to thank my parents and brother - Dr. Prashanth, for providing me with the best education possible and keeping me motivated throughout my journey. I also thank my friends in Pune and Ann Arbor for their emotional support and help.

Harsha Gouda

May 2019

Contents:

List of Figures:

List of Tables:

List of frequently used Abbreviations:

Cbl: Cobalamin

AdoCbl: 5'-deoxyadenosylcobalamin

MeCbl: Methylcobalamin

MS: Methionine synthase

MMA: Methylmalonic aciduria

M-CoA: Methylmalonyl-CoA

S-CoA: Succinyl-CoA

DMB: Dimethylbenzimidazole

MCM: Methylmalonyl-CoA mutase

ATP: Adenosine 5'-triphosphate

PPPi: Inorganic triphosphate

ATR: ATP:cobalamin adenosyltransferase

CblA: G-protein chaperone of MCM coded by the *cbl*A locus in humans

GWAS: Genome-wide association study

ITC: Isothermal calorimetry

GTP: Guanosine 5'-triphosphate

GDP: Guanosine 5'-diphosphate

GMPPCP: β,γ-Methyleneguanosine 5′-triphosphate

EPR: Electron spin resonance spectroscopy

S.A: specific activity for AdoCbl synthesis

Abstract

Humans have evolved a sophisticated trafficking pathway for absorption and utilization of a reactive and less abundant cofactor B_{12}. Methylmalonyl-CoA mutase (MCM) utilizes AdoCbl synthesized by the ATP:cobalamin adenosyltransferase (ATR) in the mitochondria to catalyze isomerization reaction of M-CoA to S-CoA crucial for odd-chain fatty acid and branch chain amino acid metabolism. S174L, R190C/H and E193K ATR patient mutation and R532H SNP variation in MCM were studied in efforts understand biochemistry of cobalamin trafficking in mitochondria. Impaired Arg190 mutant's ability to synthesis AdoCbl suggested its likely involvement in catalyzing the adenosyl transfer reaction catalyzed by ATR. ATP in addition to serving as substrate promotes formation of cobalamin binding pocket, impairment in ATP binding pocket in R190C/H and E193K mutants possibly translats into formation of defective cobalamin binding pocket displaying weaker affinity towards cob(II)alamin. Arg190 mutants have conserved ATR active site property to show stronger affinity for AdoCbl in the presence of triphosphate, but without performing any chemistry on the Co-C bond unlike wild-type ATR, invoking the importance of triphosphate in the active site. R532H variation in MCM resulting higher serum B_{12} levels show a similar substrate binding and M-CoA turnover activity like the wild-type MCM, however physiological effects of slow AdoCbl transfer from ATR to MCM in R532H variation need to be understood. These biochemical studies in addition to helping us understand the cobalamin trafficking could also assist in development of effective treatment strategy for patients born with inborn errors of B_{12} metabolism.

INTRODUCTION

Vitamin B_{12} is a complex organometallic micronutrient that is required by humans. Clinical studies on patients with the inborn errors of B_{12} metabolism have revealed various proteins involved in cobalamin absorption and trafficking in humans.[1] B_{12} is however, only used by two enzymes in mammals- methionine synthase (MS) located in the cytoplasm, and methylmalonyl-CoA mutase (MCM) in mitochondria (Figure 1). Methylcobalamin (MeCbl)-dependent MS catalyzes the conversion of homocysteine to methionine.[2] MCM uses adenosylcobalamin (AdoCbl) for the isomerization of methylmalonyl-CoA (M-CoA) to succinyl-CoA (S-CoA).[1] Clinical studies reveal that the defects associated with the MeCbl branch result in homocystinuria, whereas mutations in the AdoCbl branch result in methylmalonic aciduria (MMA).

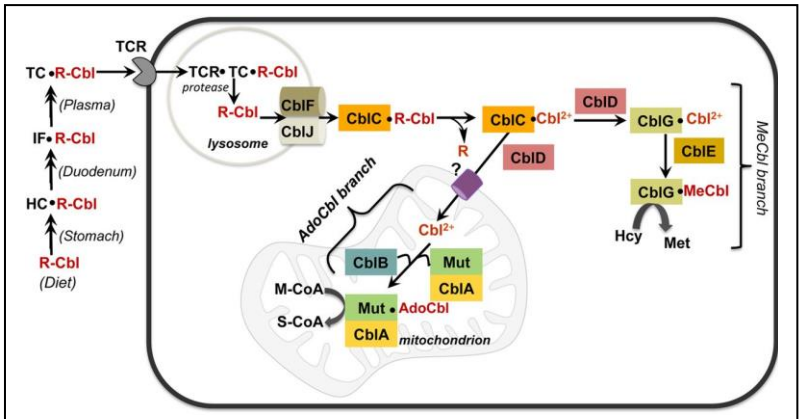

Figure 1: Outline of various proteins involved in cobalamin assimilation from diet and intracellular trafficking in humans. MeCbl and AdoCbl branches refers to cytoplasmic and mitochondrial pathways respectively. Adapted from *Carmen Gherasim et al. J. Biol. Chem. 2013; 288:13186-13193.*

Cobalamins contain a cobalt ion that is coordinated to the corrin ring. In solution, the lower or α-axial ligand position is occupied by dimethylbenzimidazole (DMB) The pKa of DMB in AdoCbl is 3.7. Hence, cobalamins in solution are predominantly found in the "base-on" conformation in which the DMB ligand is coordinated to the cobalt. Various β-axial

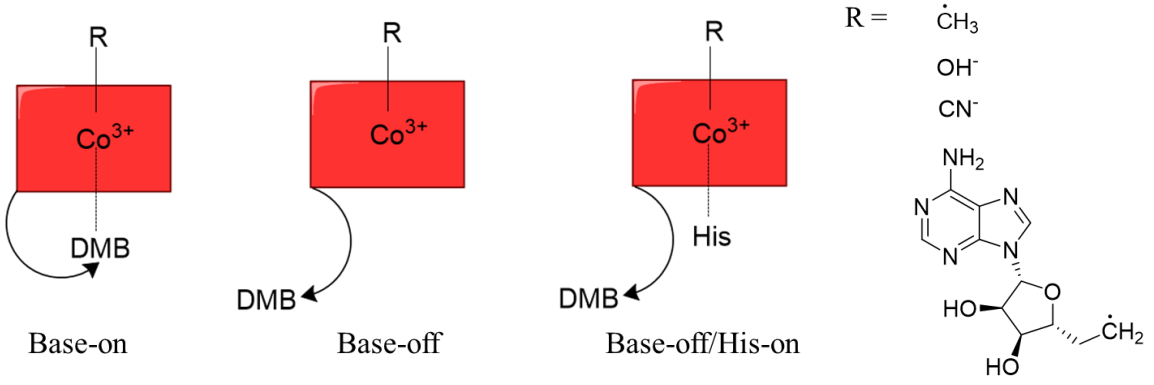

Figure 2: Different conformations of cobalamin, Histidine in the 'base-off/his-on' conformation is mostly donated by the cobalamin binding protein. 'R' represents the various β-axial ligands found in cobalamins.

ligands are seen in cobalamins including cyano- (vitamin B_{12}), methyl- (MeCbl), 5'-deoxyadenosyl- (AdoCbl) and water (OH_2Cbl). In the 'base-off' conformation the DMB ligand is protonated while in the "base-off/His-on" conformation, found in the human B_{12} enzymes, the lower axial ligand is replaced by histidine ligand.

Mitochondrial B_{12} metabolism: Proteins involved in the mitochondrial B_{12} trafficking pathway are encoded by the *cbl*A, *cbl*B and *mut* loci. Of these, the *mut* locus encodes MCM, the only mitochondrial B_{12} utilizing enzyme.[3] The substrate for MCM, *R*-methylmalonyl-CoA, is formed by carboxylation of propionyl-CoA and isomerization of the "S" to the 'R' isomer by an M-CoA epimerase.[2] MCM uses AdoCbl as a radical reservoir for catalyzing the isomerization of M-CoA to S-CoA, thus funneling catabolites of odd-chain fatty acid, branched amino acids, and cholesterol into the TCA cycle.[4,5,6] Occasionally, MCM is inactivated during the catalytic cycle when cob(II)alamin becomes uncoupled from deoxyadenosine. Inactivated MCM is repaired by the transfer of cob(II)alamin from MCM to adenosyltransferase (ATR) in the presence of a G-protein chaperone, CblA.[7,8]

ATR is encoded by the *cbl*B locus.[9] It is a multifunctional enzyme, which has the following roles. (i) AdoCbl synthesis: ATR catalyzes the adenosylation of cob(I)alamin by ATP forming AdoCbl and triphosphate.[10] **(ii)** AdoCbl loading onto MCM: ATR transfers newly synthesized AdoCbl to MCM, thus preventing the potential loss of the cofactor by releasing into solution.[11] (iii) Cob(II)alamin off-loading from MCM: ATR accepts cob(II)alamin from

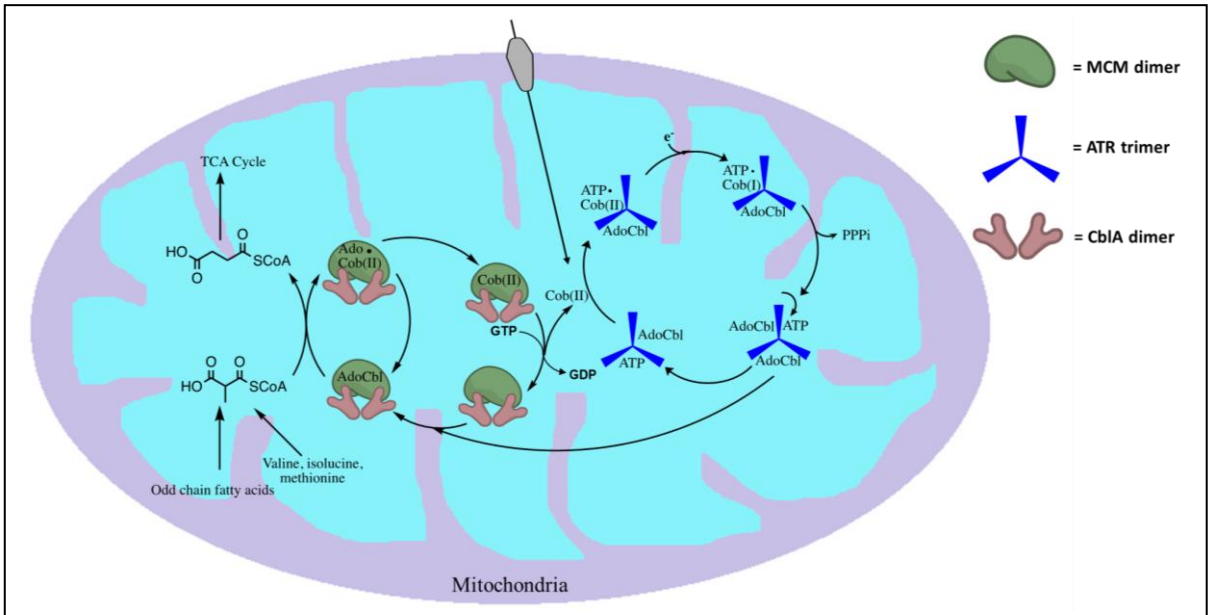

Figure 3: Role of humans mitochondrial cobalamin trafficking proteins in AdoCbl synthesis, utilization and repair. MCM plays an important role in catabolic pathways leading from odd chain fatty acids, cholesterol and branched chain amino acids to TCA cycle.

inactive MCM during the repair cycle. Both steps ii and iii require the presence of the G-protein chaperone CblA.

ATR also appears to play a role in AdoCbl sequestration if it is unable to transfer the cofactor to MCM. ATR retains the cofactor by catalyzing homolysis of the cobalt-carbon bond of AdoCbl in the presence of triphosphate forming cob(II)alamin and 5'-hydroperoxyadenosin (AdoCOOH).[12] This represents an unusual strategy since the cobalt-carbon bond in AdoCbl is formed via nucleophilic chemistry.

Structural of human ATR and MCM: Human ATR is a homotrimer with the active sites located at the trimer interfaces. Several residues in the binding interface are conserved in ATRs from different organisms and might be important for substrate binding and/or catalysis. Inherited mutations in ATR cause MMA and in this study, we report the biochemical characterization of a subset of ATR patient mutations.[13]

Human MCM is a homodimer and has a distinct binding domains for substrate and cofactor. His627 in the active coordinates the cobalt ion as the α-axial ligand while the DMB tail is buried in a hydrophobic cavity.[14] Reordering of the interdomain belt upon AdoCbl binding in MCM shields the cobalamin from the solvent . In this study, we have characterized the R532H single nucleotide polymorphic (SNP) variant of MCM. This residue is located in the interdomain connecting belt and is correlated with increased serum B_{12} levels in humans as identified by genome-wide association studies (GWAS).[15, 16]

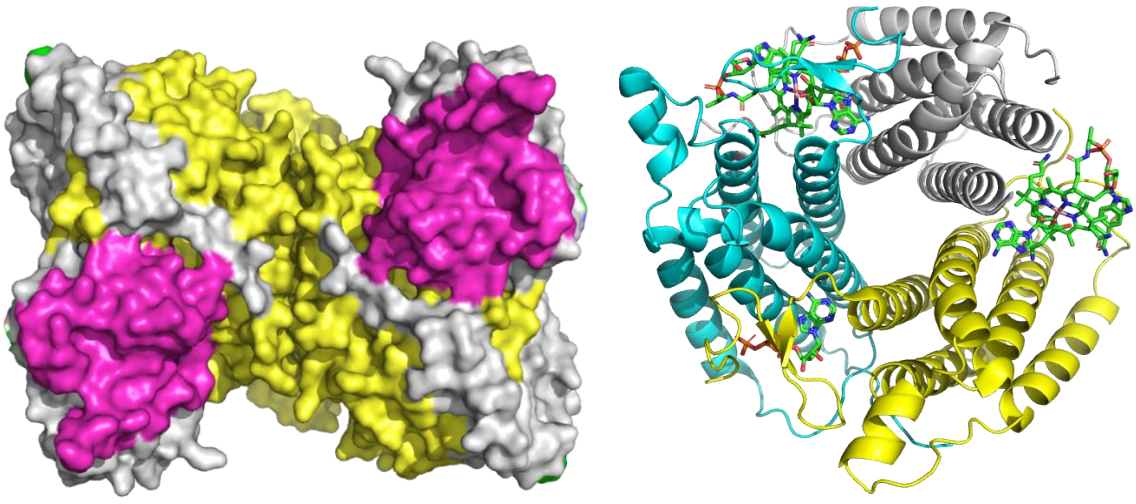

Figure 4: Structures of human MCM and ATR. *Left*. MCM homodimer (PDB: 2XIQ), with domains for M-CoA (yellow) and AdoCbl binding (magenta) connected by an interdomain belt (grey). *Right*. Each monomer in the ATR homotrimer (right, PDB: 6D5K), is represented in a different color. B_{12} and ATP are shown in stick display.

METHODS

Materials: All the primers used to generate mutations were purchased from Integrated DNA technologies. Reagents including AdoCbl, ATP, GTP, PPPi, and DTNB were purchased from Sigma-Aldrich.

Standard buffer conditions for experiments: All titration experiments unless noted otherwise, were performed in 50 mM HEPES pH 7.5, containing 150 mM KCl, 2 mM $MgCl_2$, 2 mM TCEP and 5% glycerol, which is designated as Buffer A.

Purification of wild-type and mutant human ATR: The ATR expression clone in a pET-28b vector containing thrombin-cleavable N-terminal His-tag was transformed into BL21 (DE3) *E. coli* cells*. A* single transformant was inoculated into 100 ml of Luria broth (LB) medium containing 50 μg/ml of kanamycin and was grown overnight at 37 °C. Approximately 10 ml of culture was inoculated into one liter of LB and expression of recombinant ATR was induced with 50 μM IPTG when cells reached an OD_{600nm} of 0.6. The cells were left to grow overnight at 20 °C and were harvested the next day by centrifuging at 4,200 rpm for 20 mins.

The cell pellet was resuspended in lysis buffer containing 50 mM Tris pH 8.0 containing 300 mM NaCl, 10 mM imidazole and 1 mM TCEP. Cells were disrupted by sonication and the lysate was centrifuged at 17,000 rpm. The supernatant was loaded onto a 25 ml Ni(II)-NTA column. ATR was eluted using a 200 ml linear gradient of imidazole ranging from 10- 200 mM in the lysis buffer. The N-terminal His-tag on ATR was cleaved by adding thrombin (5 units/mg protein) and by dialyzing the protein overnight at 4 °C in lysis buffer. ATR was loaded onto a second 25 ml Ni(II)-NTA column and eluted using lysis buffer. Thrombin was removed by eluting ATR in a 5 ml Benzamidine column (GE healthcare) with 25 mM HEPES pH 7.4, 500 mM NaCl, 1 mM TCEP. ATR was then dialyzed overnight against 50 mM HEPES pH 7.5, containing 150 mM KCl, 2 mM $MgCl_2$, 2 mM TCEP and 5% glycerol, and was stored at -80 °C.

Mutant	Forward primer
R190H	5’-GCCGTGTGVCATCGGGCCGAG -3’
R190C	5’-CTCGGCCCGACAGCACACGGC -3’
E193K	5’-TGCCGCCGGGCCAAAAGACGTGTGGTG- 3’
S180W	5’-GGCAAGATCAGCTGGGCGCTGCATTTC-3’
S174L	5’-GCCTTCATCCTGCCTCTGGGAGGCAAGATCAGC-3’

The desired patient mutations were generated using the following forward primer sequences and reverse primers with complementary sequences. The mutations were confirmed by nucleotide sequencing at Biomedical DNA sequencing core facility at Michigan medical school, Ann arbor. Mutant ATR proteins were purified like wild-type ATR.

AdoCbl binding to ATR: To monitor AdoCbl binding increasing concentrations of, wild-type or mutant ATR were added to 30 μM AdoCbl in Buffer A. The spectrum after each addition was recorded to monitor binding. The concentration of AdoCbl was determined using ε_{522nm}= 8.0 cm^{-1} mM^{-1}. The change in absorbance at 455 nm corresponded to AdoCbl bound to ATR and was plotted against ATR concentration. The data were fitted using Dynafit software (BioKin)[17] for a single binding site per monomer to determine the dissociation constant for AdoCbl binding. To monitor AdoCbl binding in the presence of inorganic triphosphate (PPPi), the above titration was performed in the presence of 1 mM PPPi.

Cob(II)alamin binding to ATR: To monitor cob(II)alamin binding, the titration was performed in an anaerobic chamber (<0.2 ppm O_2 levels). Wild-type or mutant ATR was titrated into 30 μM cob(II)alamin and 1 mM ATP in Buffer A The concentration of cob(II)alamin was determined using ε_{474nm}= 9.2 cm^{-1} mM^{-1}. The change in absorbance at 464 nm corresponding to ATR-bound cob(II)alamin was plotted against ATR concentration. he data were fit using the Dynafit software for a single binding site per monomer to determine the dissociation constant for cob(II)alamin binding to ATR.

AdoCbl synthesis by ATR: To determine AdoCbl synthesis by ATR mutants, cob(II)alamin in Buffer A was reduced to cob(I)alamin with ~10 equivalents of titanium citrate under strictly anaerobic conditions, followed by addition of 1 mM ATP and 1 μM ATR trimer to initiate AdoCbl synthesis. The concentration of cob(I)alamin was estimated using ε_{386nm}= 28.0 cm^{-1} mM^{-1}. The rate of AdoCbl synthesis was determined by measuring the change in absorbance at 522 nm .

Purification of wild-type and R532H MCM: A synthetic gene for human MCM that was codon optimized for *E. coli* expression was obtained from Genscript and cloned into the pET28b vector using the Nco I and Xho I restriction sites. The construct contains a TEV-cleavable C-terminal His-tag. Recombinant human MCM was expressed in terrific broth with the exception that 3% DMSO was added following 50 μM IPTG addition when cells reached an OD_{600nm} of 1.2 to improve protein solubility. After harvesting, cells were resuspended in 50 mM Tris-HCl, pH 8.0, containing 500 mM NaCl, 20 mM imidazole and 5% glycerol and lysed by sonication. The lysate was centrifuged at 17,000 rpm for 20 mins and supernatant was loaded onto a 25 ml Ni(II)-NTA column and eluted using a 250 ml linear gradient ranging from 20-200 mM imidazole in the same buffer. Next, the C-terminal His tag was

cleaved using His-tagged TEV protease (1:50 (m/m) TEV**:** MCM) overnight at 4 °C. The next day, more TEV protease (1:100 (m/m) TEV**:** MCM) was added to the mix and cleavage was continued under the same condition overnight. TEV protease was removed by passing through a Ni(II)-NTA column, and the flow-through was collected. The cleaved MCM protein was then loaded onto a Source Q column (Omnifit) equilibrated with 50 mM HEPES pH 7.3, 25 mM NaCl, 5% glycerol. MCM was eluted with a linear gradient of 25-500 mM NaCl in the same buffer. Purified MCM was dialyzed against 50 mM HEPES, pH 7.5 buffer containing 150 mM KCl, 2 mM $MgCl_2$, 2 mM TCEP and 5% glycerol and was stored at -80 °C.

The SNP variant of human MCM was generated using a forward primer 5'-CTGGCTGAACACTGCCTGGCAGC-3' and a reverse primer with a complementary sequence. The SNP variant protein was expressed and purified as described for wild-type MCM.

EPR spectroscopy: EPR spectroscopy to determine cob(II)alamin conformation bound to E193K mutant was performed on a Bruker ELEXSYS E500 EPR spectrometer using a Bruker ER4123SHQE X-band cavity resonator, and Bruker ER4131VT system for temperature control.[18] Samples were prepared containing 200 µM cob(II)alamin, 1.5 mM E193K ATR mutant protein and 2 mM ATP or 100 µM cob(II)alamin in 50 mM HEPES pH 7.5, 150 mM KCl, 2mM $MgCl_2$, 2 mM TCEP and 10% glycerol. Microwave frequency, 9.46 GHz; power, 2.0 mW; modulation amplitude, 1.0 mT; modulation frequency, 100 kHz; temperature, 80 K were used to acquire EPR spectra. Each spectrum represented were subtracted from the baseline buffer spectrum after acquiring average of 5 scans for each sample.

Thermal denaturation: Thermal denaturation of wild-type and R532H MCM was monitored in 250 µl samples containing 10 µM MCM in 50 mM HEPES, pH 8.0, 150 mM KCl, 2 mM $MgCl_2$, 2 mM TCEP and 5% glycerol. Absorbance at 600 nm was monitored using a spectrophotometer and the temperature of the cuvette holder was increased from 25°C to 65 °C in 5˚ increments. The samples were incubated for 5 min between at each temperature before the absorbance was monitored. The fractional change in absorbance was a function of temperature was plotted to obtain the thermal melting temperatures (T_m).

AdoCbl binding to MCM: To monitor AdoCbl binding to MCM, wild-type and R532H MCM were titrated against ~30 µM AdoCbl in 50 mM HEPES, pH 8.0, 150 mM KCl, 2 mM $MgCl_2$, 2 mM TCEP and 5% glycerol. The change in absorbance at 563 nm was plotted against the concentration of MCM. The data were fit using Dynafit software (BioKin)[17] for a single binding site per monomer to determine the dissociation constant for AdoCbl.

Thiokinase assay: The catalytic activity for MCM was monitored in a coupled thiokinase assay. For this, 20 μM MCM and 20 μM AdoCbl in standard buffer were preincubated at 30°C for 10 mins. The assay was performed in buffer containing 500 μM methylmalonyl-CoA, 3 mM $MgCl_2$, 3 mM GDP, 70 μM DTNB and 20 μg of thiokinase. The background thiokinase activity was monitored for 4-6 min prior to initiating the reaction with the mixture containing 3 μM AdoCbl and 4 nM MCM. The change in absorbance at 412 nm (ε= 14,150 M^{-1} cm^{-1}) corresponding to formation of the TNB anion, was monitored to determine the activity of MCM as described previously.[19]

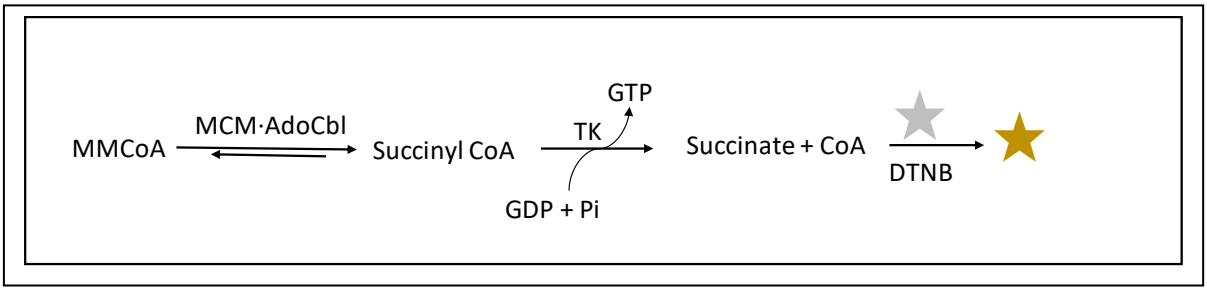

Size-exclusion chromatography: To monitor complex formation between MCM and CblA, samples containing 50 μM wild-type or R532H MCM, 100 μM CblA and 500 μM GDP, GMPPCP and GTP were injected onto a Superdex 200 column (GE Life Sciences) and eluted with buffer containing 50 mM HEPES pH 8, 150 mM KCl, 2 mM $MgCl_2$, 2 mM TCEP and 5% glycerol. Molecular weight was estimated from the elution volumes using calibration standards (Bio-Rad S200 protein standards).

GTPase activity of CblA: To determine the GTPase activity of CblA and GAP activation by MCM, samples with increasing ratios of MCM:CblA (0.5:1 to 10:1) were prepared using a fixed concentration of CblA (5 μM) in buffer containing 50 mM HEPES, pH 7.5, 150 mM KCl, 2 mM $MgCl_2$, 2 mM DTT in a total volume of 125 ml. GTP (3 mM) was added to each sample to initiate GTP hydrolysis at 30°C. Aliquots (50 μl) were removed after 10 and 20 mins and quenched by adding 2.5 μl of 2M trichloroacetic acid. The samples were centrifuged for 10 min in a table top centrifuge at maximum speed. The supernatant was diluted 1:1 with 50 mM potassium phosphate buffer, pH 6.0 containing 4 mM tetra-n-butylammonium bromide. Samples were injected onto an HPLC column (C_{18}, 4.6 mm x 25 mm) and eluted with buffer containing 50% methanol in 25 mM potassium phosphate buffer, pH 6.0 and 2 mM tetra-n-butylammonium bromide. The concentration of GDP was estimated by integration of the peak area as described previously .[20]

AdoCbl transfer from ATR to MCM: To monitor AdoCbl transfer from ATR to MCM, 45 μM wild-type ATR in 50 mM HEPES buffer pH 7.5 containing 150 mM KCl, 2 mM $MgCl_2$, 2 mM TCEP and 5% glycerol was mixed with 15 μM AdoCbl to load approximately one binding site

per trimer. MCM (30 μM) and CblA (90 μM) in the same buffer was added to initiate the transfer reaction. Spectra were recorded at 30 ˚C over 80 min. The rate of AdoCbl transfer was determined by fitting the change in absorbance at 530 nm to a double exponential equation using Origin lab software.

3. RESULTS AND DISCUSSION

3.1. Biochemical studies on human ATR patient mutations

A subset of ATR mutations that have been described in *cblB* patients with methylmalonic aciduria were characterized biochemically.[13] The selected missense mutations were located at or near the enzyme active site and predicted to influence substrate binding and/or catalytic activity. Two of the altered residues Arg190 and Glu193 interact via hydrogen bond and ionic interactions with ATP. Arg186 forms an inter-subunit salt bridge with Asp90 in the adjacent monomer, only when cobalamin is bound. Residues Ser174, Ser180, Gln234 and Gly97 are located in a hydrophobic region below the cobalamin binding site. F170 located in this same region is presumed to play an important role in maintaining cobalamin in the base-off conformation. Residue Arg191 located facing away from the active site is predicted to engage in interactions crucial for trimer formation (Figure 5).

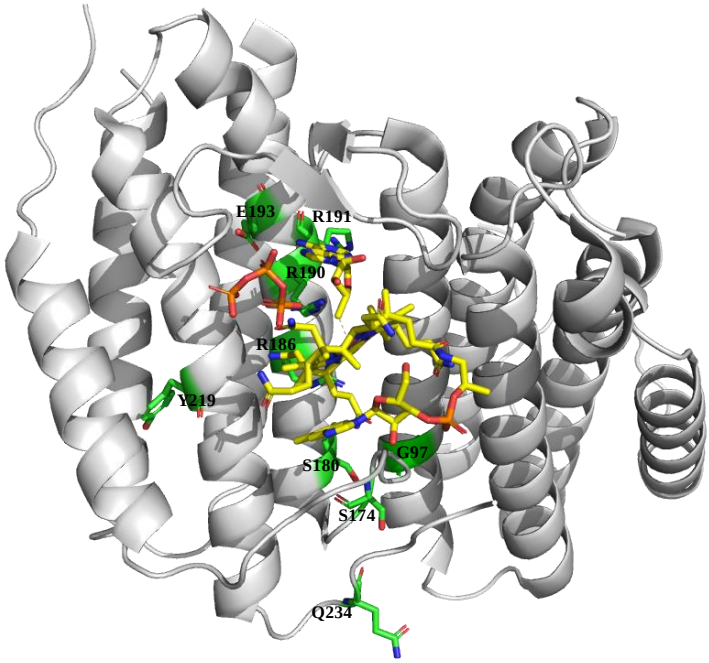

Figure 5: Mapping of identified *CblB* patient mutations to ATR active site (PDB:6D5X).

Patient mutations S174L, S180W, R186Q, R190C, R190H, and E193K were generated by site-directed mutagenesis. Wild-type and mutant ATR proteins were expressed and purified as described in the Methods section. With the exception of S180W and S174L, the remaining mutants were soluble. Since S180W was completely insoluble, it could not be characterized. S174L ATR was partially insoluble after lysis but was obtained in sufficient amounts to support its characterization.

a. Monitoring impact of patient mutations on ATP binding to ATR

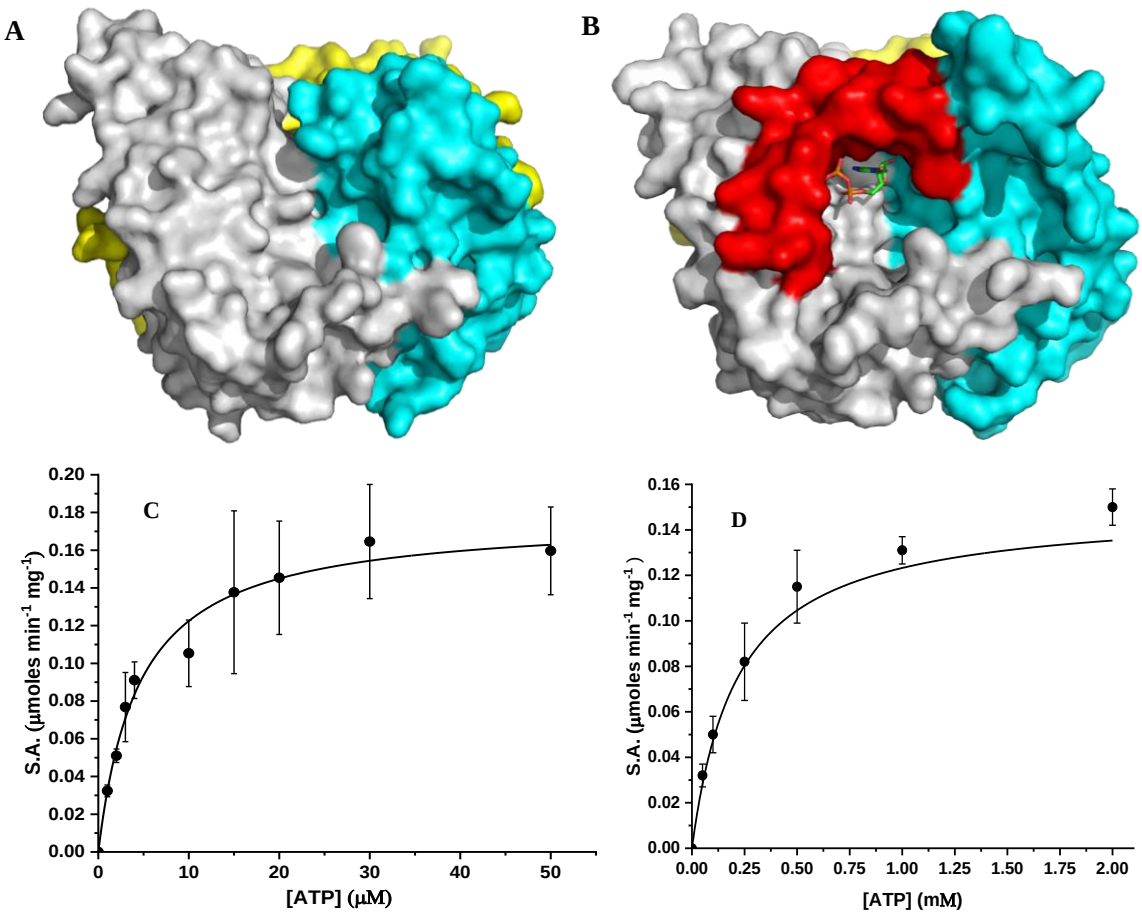

Figure 6: a) Structure of apo-ATR active site, b) ATP binding to ATR promotes organization of N-terminal residues (red) and promotes formation of cobalamin binding pocket. Michaelis-Menten plot of AdoCbl synthesis at variable ATP concentrations for wild-type (c) and E193K mutant (d).

ATP binding to ATR active site in the trimer interface is a paramount step in the mechanism of AdoCbl synthesis on ATR and is stabilized by multiple noncovalent interactions in the active site. Crystal structure of ATP bound human ATR display that only two of the three active sites are in an ATP bound state with the other remaining unliganded. ATP presumably binds ATR inserting adenosine ring deep into the active site facing C5'-carbon towards the cobalamin binding site and phosphate group projecting outwards. Comparison of the ATP bound active site to apo-active site reveals that ATP binding influences the ordering of the N-terminal residues in the active site and also promote the formation of the oval-shaped active site cleft measuring 14 X 8 Å and 7 Å depth resulting to the formation of cobalamin binding site for catalysis.[21] In spite of multiple efforts to determine ATP binding to R190C, R190H and E193K mutations by isothermal calorimetry (ITC), we failed to observe heat exchanges that could correspond to ATP binding in the mutant ATR

proteins. The AdoCbl synthesis activity of mutant proteins encouraged us determining the Michaelis-Menton constant (K_m) that could help us understand the impairment of ATP binding in ATR mutants. The kinetic constant K_m was determined by measuring Adocbl synthesis activity at variable concentrations of ATP in wild-type and mutant proteins and fitting the data to the Michaelis-Menten equation using OriginLab software. The K_m value for ATP in wild-type (K_m = 4.5 ± 1.1 µM) indicated that ATR binds ATP in micromolar affinities and will always be in ATP bound state *in-vivo* as a result of high ATP concentrations (~5mM) in physiological conditions. S174L patient mutation, located quite far away from the ATP binding site didn't impair Michaelis-Menton constant for ATP binding. Wherein we found that mutations R190C and E193K mutant proteins have moderately impaired ATP binding reducing K_m to the submillimolar range. Despite changes in K_m value for ATP in the R190C and E193K mutants, it is very less likely to have a physiological impact on AdoCbl synthesis in the patients due to high concentrations of ATP in the cell. As ATP binding in wild-type ATR results in conformational change forming a cobalamin binding pocket. It possible that impairment in ATP binding is not providing adequate ligand binding energy in mutant proteins for the formation of appropriate cobalamin binding pocket, resulting in the impaired cob(II)alamin binding.

Table 1: Michaelis-Menten constant for ATP of wild-type and mutants. Specific activity (S.A.) and k_{cat} for AdoCbl synthesis turnover at V_{max} conditions.

ATR	K_m (ATP)	S.A. (µmoles min^{-1} mg^{-1})	k_{cat} (min^{-1})
Wild type	**4.5 ± 1.1 µM**	**0.18 ± 0.01**	**14.8 ± 3.5**
S174L	**4.5 ± 0.7 µM**	**0.25 ± 0.01**	**18.6 ± 0.9**
R190C	**N.D**	**0.01 ± 0.01**	**0.1 ± 0.1**
R190C	**92.3 ± 30.7 µM**	**0.01 ± 0.01**	**0.7 ± 0.1**
E193K	**235.2 ± 15.6 µM**	**0.16 ± 0.01**	**9.5 ± 0.4**

b. Monitoring impact of patient mutations on cob(II)alamin binding to ATR

Following from the previous section that ATP binding to ATR promotes the formation of cobalamin binding pocket, hence cob(II)alamin bind to ATR in an ATP dependent manner and exhibit weak binding in the absence of ATP. Cob(II)alamin is a biradical form of the cofactor B_{12} that's reactive to oxygen and forms aquocobalmin in aerobic conditions. ATR binds cob(II)alamin in a similar 'base-off' conformation like the AdoCbl, cob(II)alamin binding was monitored by UV-vis spectroscopy observing the increase in extinction co-efficient at 464 nm upon cob(II)alamin binding to ATR in the anaerobic conditions ($[O_2] < 0.2$ ppm).[22] Base-off conformational binding of cob(II)alamin on ATR significantly reduces the reduction potential for conversion of cob(II)alalmin to cob(I)alamin that's required for the subsequent nucleophilic attack on C5'-carbon of ATP for the adenosyl transfer reaction.[23] Base-off conformational binding of cobalmin facilitating the reduction of cobalt on ATR suggests that cob(II)alamin is likely to be an ATR substrate in the physiological conditions before its reduction to cob(I)alamin.

ATR patient mutant proteins were characterized for cob(II)alamin binding similar to wild-type in the presence of 1 mM ATP in anaerobic conditions. S174L, R190H, and R190C mutant proteins exhibit a similar spectroscopic change implying the formation 'base-off' four-coordinate conformation like the wild-type ATR. Binding dissociation constant (K_d) for cob(II)alamin in S174L mutation was in submicromolar concentrations similar to wild-type ATR, whereas R190H and R190C mutations exhibit weaker affinity in micromolar range compared to wild-type. It is interesting to notice R190C/H and E193K mutations that impair the ATP binding also impair cob(II)alamin binding having no direct contacts to the cobalamin binding site, implying that importance of ATP binding in forming cobalmin binding pocket.

Table 2: Cob(II)alamin binding dissociation constants and its binding conformation to wild-type and mutant ATR proteins.

hATR mutant	K_d (μM)	Conformation
WT ATR	0.08 ± 0.01	Base-off
S174L	0.42 ± 0.28	Base-off
R190C	38.5 ± 16.5	Base-off
R190H	46.0 ± 10.0	Base-off
E193K	N.D	Base-off

In efforts to identify the cob(II)alamin binding conformation in E193K mutant ATR, similar titration experiments were performed in the presence of 2 mM ATP; it was unusual to observe no spectroscopic change upon E193K addition to cob(II)alamin. To determine binding of cob(II)alamin to E193K mutant, sample with 100 μM cob(II)alamin, 1.5 mM E193K ATR and 2 mM ATP was centrifuged through the 10K Da separation tube (Life Sciences) to

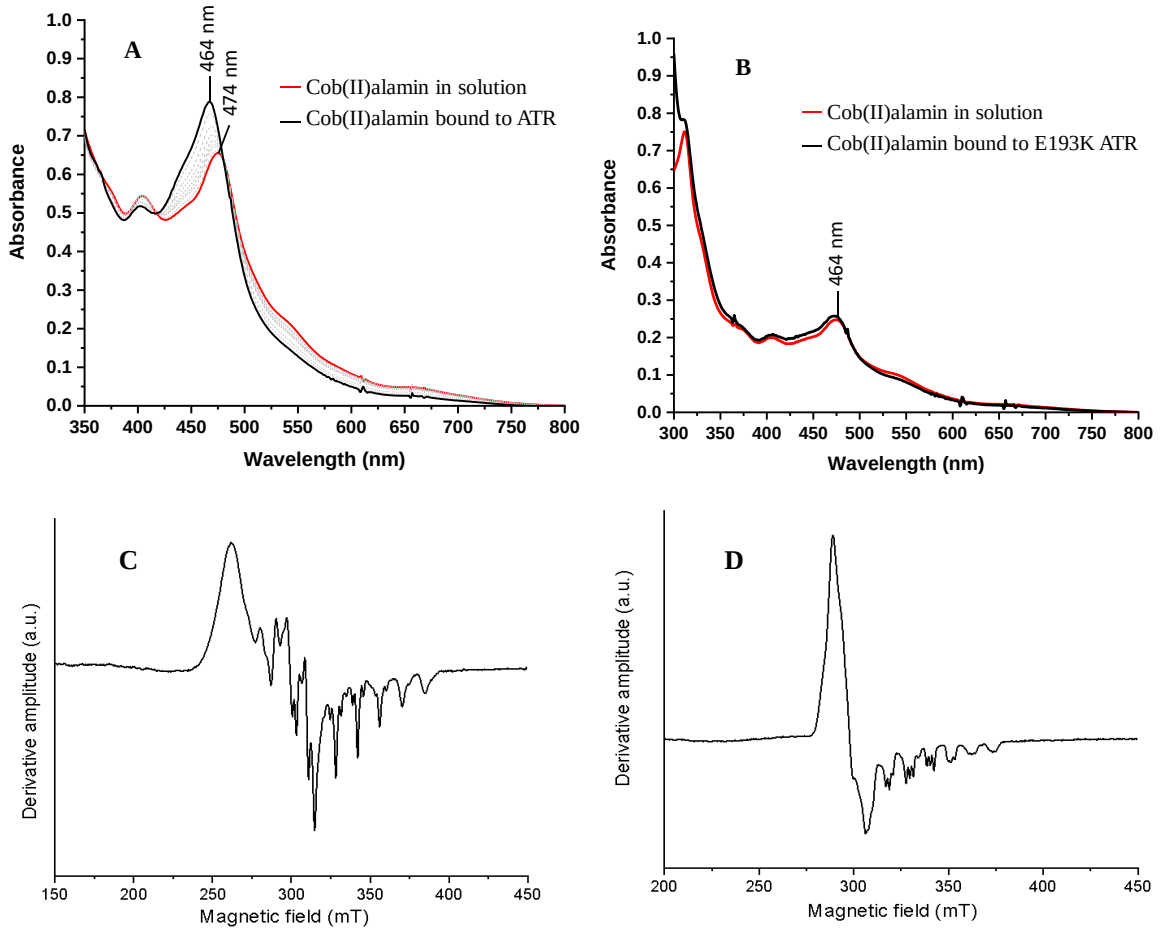

Figure 7: a) Monitoring cob(II)alamin binding to wild-type and mutant ATR, b) Monitoring cob(II)alamin binding to E193K ATR mutant. red: five-coordinate cob(II)alamin in solution, black: four-coordinate cob(II)alamin bound to ATR. c) EPR spectrum of cob(II)alamin bound to E193K mutant, d) EPR spectrum of 'base-on' conformation cob(II)alamin in solution.

confirm binding. We hypothesised that either of the following could be a plausible reason for the observed no change in spectrum (i) The cob(II)alamin bind E193K mutant protein in a 'base-on' conformation unlike wild-type ATR or (ii) The electronic environment resulting in increased extinction coefficient at 464 nm absorption upon cob(II)alamin binding to wild-type is perturbed in E193K mutation. In efforts to identify the cob(II)alamin binding conformation on E193K ATR, we were able to perform an electron spin resonance (EPR) spectroscopy for the E193K ATR bound cob(II)alamin. Cobalt nuclei in cob(II)alamin gives eight signals (I=7/2) as a result of electron-nuclei hyperfine interaction.[24,25] Cob(II)alamin five-Coordinate 'base-on' conformation in solution results in further splitting of lines into three components due to hyperfine coupling with nitrogen (I=1) nuclei of ^{14}N coordination from the DMB ligand. The absence of hyperfine splitting by nitrogen nuclei in EPR spectra of cob(II)alamin bound to E193K mutant implied that cob(II)alamin is bound in a base-off conformation to a mutant protein similar to wild-type but has no spectroscopic changes to monitor binding by UV-vis

spectroscopy[24] (Figure 10).The EPR spectrum of cob(II)alamin bound to E193K ATR resembles the spectrum of five-coordinate cob(II)alamin, water serving as its fifth ligand implying the perturbation of cobalamin binding site in E193K ATR mutant.[24] Formation of five-coordinate cob(II)alamin on E193K ATR is likely to be physiologically relevant as the water coordination has an effect on the reduction potential of cob(II)alamin.

c. Determining the impact of patient mutations on AdoCbl synthesis activity of ATR

ATR is an ATP-dependent adenosyltransferase and converts cob(I)alamin into an AdoCbl that is utilized by MCM as a cofactor. Although the mechanism of cobalamin uptake into the mitochondrial matrix remains to be elucidated, human ATR binds cob(II)alamin with a K_d of 0.08 μM in the presence of ATP.[12] Binding cob(II)alamin in the base-off state is known to reduce the cob(II)alamin/cob(I)alamin reduction potential.[22] Following reduction, the resulting cob(I)alamin which is a supernucleophile attack the C5'-carbon of ATP resulting in adenosyl transfer to form AdoCbl and PPPi.

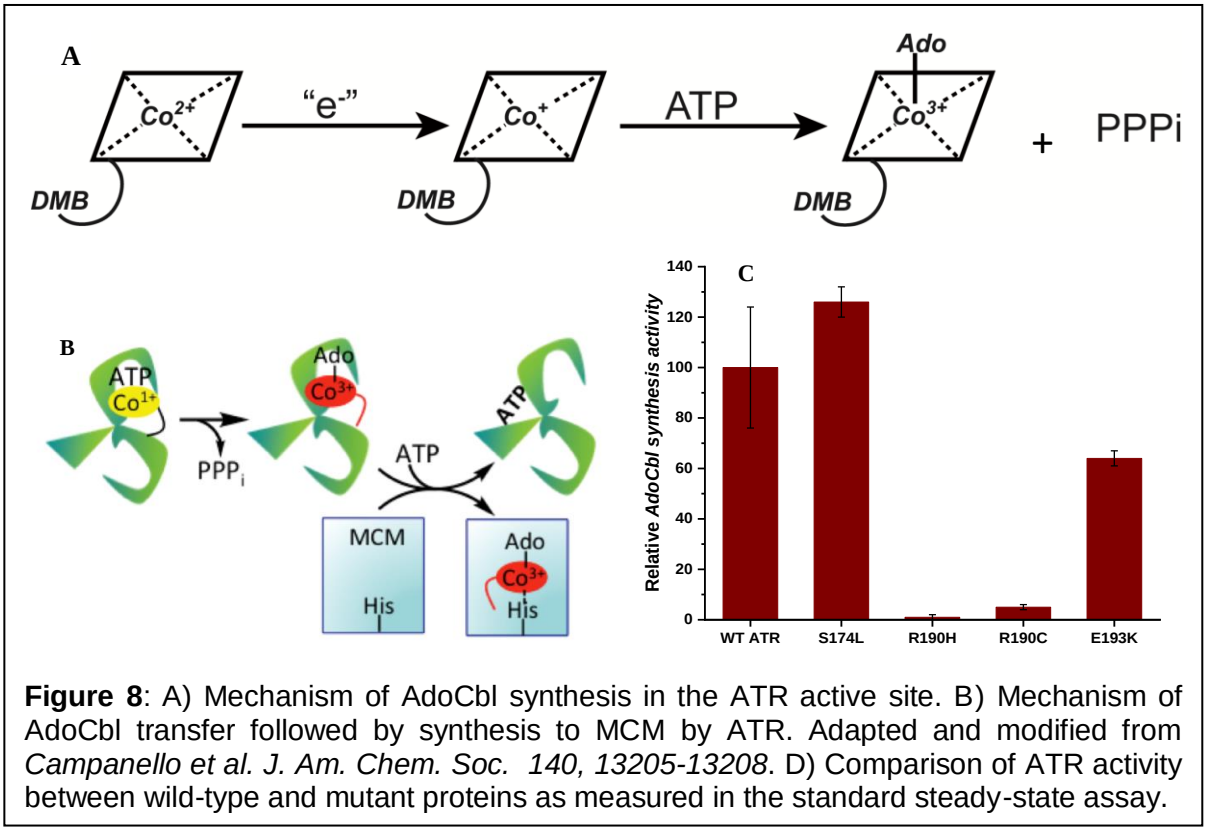

Figure 8: A) Mechanism of AdoCbl synthesis in the ATR active site. B) Mechanism of AdoCbl transfer followed by synthesis to MCM by ATR. Adapted and modified from *Campanello et al. J. Am. Chem. Soc. 140, 13205-13208*. D) Comparison of ATR activity between wild-type and mutant proteins as measured in the standard steady-state assay.

Purified mutant proteins were evaluated for their AdoCbl synthesis activity in the anaerobic chamber using Ti(III)citrate as an artificial reductant to reduce cob(II)alamin to cob(I)alamin. Increase in 522 nm absorbance corresponding to AdoCbl maxima in solution was monitored to determine the rate of AdoCbl synthesis in wild-type and mutant proteins. Mutations E193K and S174L proteins show similar catalytic rate like wild-type, while Arg190 mutants are found to have greatly reduced catalytic efficiency in comparison to wild-type for

the AdoCbl synthesis (Table 1 shows the specific activity and k_{cat} for AdoCbl synthesis for wild-type and mutants). The reduced activities in R190C and R190H mutants suggested Arg190 residue is likely involved in catalyzing the Adenosyl transfer reaction in wild-type ATR.

Arg190 residue in the active site forms noncovalent interactions with ATP upon binding (Figure 7). The nitrogens of the guanidinium group in arginine interact with the oxygen of the ribose ring and the oxygens of α-phosphate in ATP and stabilize its binding. These electrostatic or hydrogen bonding interactions in the active site are likely to play a vital role in positioning the C5'-carbon of ATP towards cobalamin binding site for catalyzing adenosyl transfer reaction in the ATR active site. Mutations in residue Arg190 plausibly results in aberration of these interactions to hold C5'-carbon in the appropriate orientation resulting in their reduced AdoCbl synthesis activity. It is also interesting to note how the change in Arg190 mutation either to cysteine or histidine residue also has a minor effect on the catalytic activity of an enzyme.

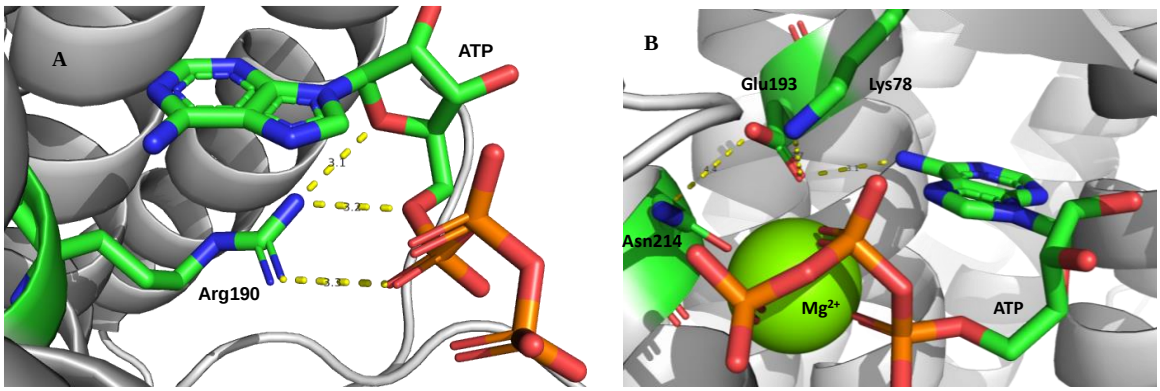

Figure 9: Arg190 (a) and Glu193 (b) residue interactions in active site. Dashed lines (yellow) indicate the possible non-covalent and ionic interactions.

d. Triphosphate increases ATR affinity for AdoCbl

In the presence of apo-MCM, the newly formed AdoCbl is transferred directly from ATR without releasing into solution.[11] However, in the absence of MCM, AdoCbl and PPPi in the active site catalyze the formation of an intermediate of weakened Co-C bond. Intermediate fosters homolysis of Co-C bond in aerobic condition to form cob(II)alamin on ATR releasing 5'-hydroperoxyadenosin ($AdoCH_2OOH$). Kinetic values AdoCbl transfer (0.63 min^{-1}) and homolysis (0.082 min^{-1}) reactions chiefly suggest that AdoCbl transfer onto MCM is favored over Co-C bond homolysis.[12] Homolysis of Co-C bond results in the retention of tightly bound cofactor form cob(II)alamin on ATR in the absence of MCM. The AdoCbl (λ_{max} = 522 nm) binding from solution to ATR (λ_{max} = 455 nm) shows large blue shift that could be

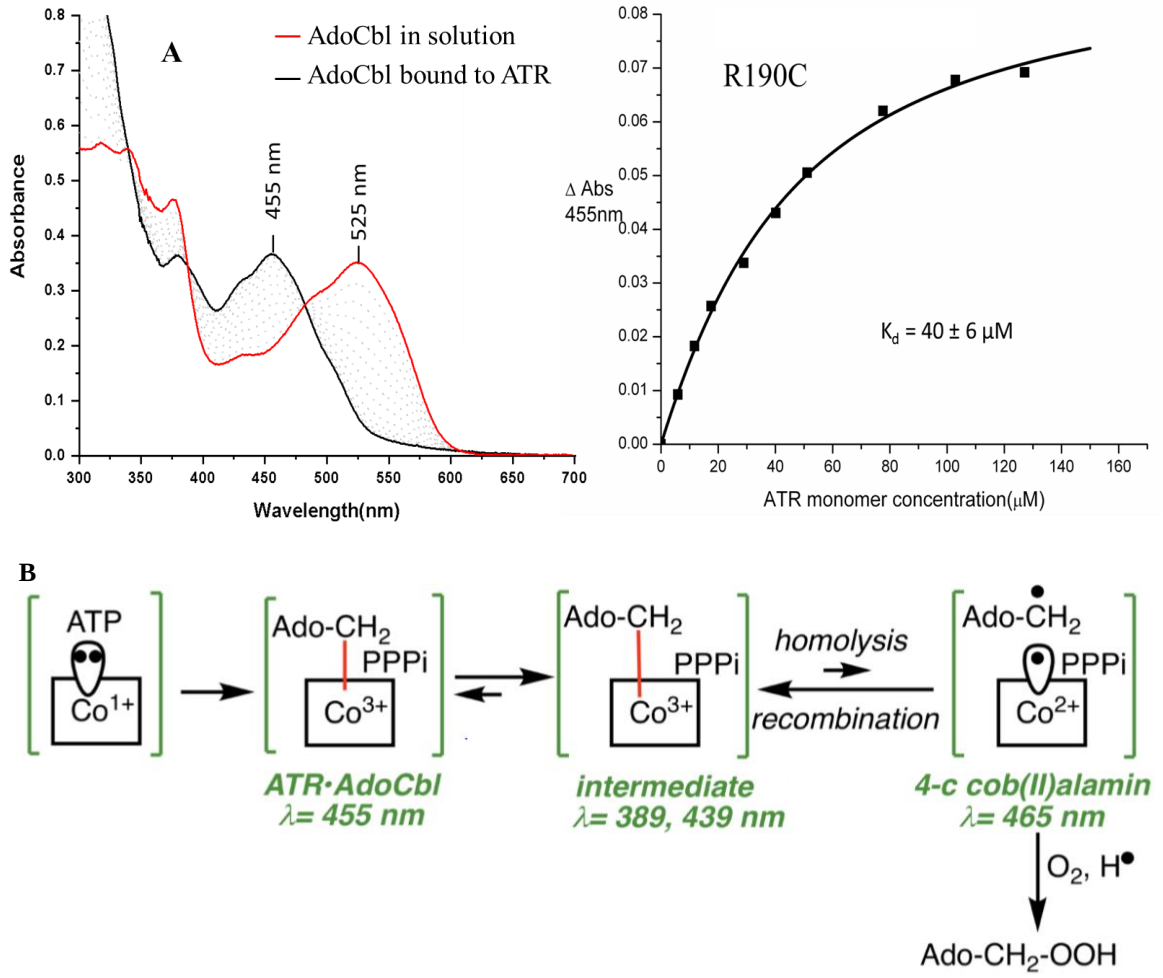

Figure 10: A) Monitoring AdoCbl binding to wild-type ATR and the mutants (left). red: AdoCbl in base-on conformation in solution, black: AdoCbl in base-off conformation bound to ATR. Change in 455 nm absorbance was plotted using dynafit for one binding site per monomer to determine binding dissociation constant (K_d) for R190C mutant in the absence of triphophate (right). B) showing the mechanism of conversion of AdoCbl to cob(II)alamin in the presence of PPPi in the active site. Adapted and modified from *Campanello et al. J. Am. Chem. Soc. 140, 13205-13208*.

monitored using UV-vis spectroscopy to determine the binding of AdoCbl to ATR.[25] AdoCbl binds ATR in a 'base-off' conformation in a five-coordinate state in contrast to its mitochondrial partner protein MCM, that binds cofactor in a 'base-off/His-on' confirmation.[26] As a synthesis of AdoCbl is accompanied by the formation of triphosphate in the active site, we also tested the effects of AdoCbl binding in triphosphate presence by performing similar titration experiments in the presence of 1 mM inorganic triphosphate. The data was fit for one binding site per monomer to determine the dissociation constant (K_d) for AdoCbl binding in wild-type and mutant proteins both in the presence and absence of 1 mM triphosphate. We observed wild-type human ATR bind AdoCbl in the absence of triphosphate in a micromolar affinity and has an increased affinity for AdoCbl in the presence of triphosphate accompanied by chemistry forming a weakened Co-C bond intermediate. Presence of

Table 3: AdoCbl binding dissociation constants, binding conformations and Co-C bond homolysis for wild-type and ATR mutants in the presence and absence of 1 mM inorganic triphosphate.

Mutant	Titration	K_d (μM)	Conformation	Co-C homolysis
WT	- PPPi	1.0 ± 0.3 μM	Base-off	Yes
	+ PPPi	0.2 ± 0.1 μM		
S174L	- PPPi	3.8 ± 0.3 μM	Base-off	Yes
	+ PPPi	0.4 ± 0.2 μM		
R190H	- PPPi	50 ± 5 μM	Base-off	No
	+ PPPi	13 ± 3 μM		
R190C	- PPPi	40 ± 6 μM	Base-off	No
	+ PPPi	4 ± 1 μM		
E193K	- PPPi	120 ± 30 μM	Base-off	No
	+ PPPi	100 ± 30 μM		

triphosphate in the active site changes the UV-vis spectrum of five-coordinate AdoCbl bound to ATR (λ_{max} = 439 nm) as a result of the formation of weak Co-C bond intermediate. ATR mutants S174L, R190C, R190H and E193K bind AdoCbl in the 'base-off' conformation similar to wild-type ATR, but show a weaker affinity towards the AdoCbl compared to wild-type. Mutation S174L located farther away from the ATP active site does Co-C bond homolysis similar to wild-type, wherein the R190C, R190H and E193K mutants failed to form a weakened Co-C bond intermediate and perform Co-C bond homolytic chemistry. But, the tendency to show increased affinity for the AdoCbl in the presence of triphosphate was still retained in R190H and R190C mutants without having to perform any Co-C homolytic chemistry is interesting. Mutant E193K ATR neither showed any Co-C bond homolysis nor increased affinity for the cofactor in the presence of 1 mM inorganic phosphate implying the flaws or no PPPi binding in the E193K patient mutation. Weak binding of AdoCbl in R190H, R190C, and E193K mutants is likely to result in the release of cofactor into mitochondrial matrix *in-vivo* resulting in its loss by dilution, wherein wild-type ATR could retain cofactor in the active site by forming cob(II)alamin in the absence of apo-MCM. It would be interesting to look into the thermodynamics of AdoCbl binding in the presence and absence of PPPi using isothermal calorimetry (ITC) to determine free energy changes affected by the absence of PPPi in wild-type, R190C and R190H ATR.

e. Conclusions and future perspectives

These studies on human ATR mutations have helped us understand the possible biochemical penalties associated with these patient mutations resulting in methylmalonic aciduria. Perturbed R190H and R190C mutants ability to synthesize AdoCbl suggesting Arg190 residues critical role in the active site and could likely be a catalytic residue orienting the C5'-carbon of ATP towards the cob(I)alamin favoring the nucleophilic adenosyl transfer reaction. We also observed fascinating biochemistry in regards to AdoCbl binding in Arg190 mutations, In the presence of an inorganic triphosphate in the active site the mutant proteins exhibit tighter affinity towards AdoCbl similar to wild-type without having to form any Co-C bond chemistry unlike in the wild-type. Further thermodynamics studies on AdoCbl binding to wild-type and Arg190 mutants in both presence and absence of triphosphate would give us new insights into the understanding of inorganic triphosphate role in the active site resulting to weakened Co-C bond and tightened AdoCbl binding. We believe that the Arg190 mutants weak affinity for Cob(II)alamin togeather with their low AdoCbl synthesis activity could result in their observed phenotype causing methylmalonic aciduria. The mutation E193K modifies the structure of the ATP binding site as mutation brings the inversion of the electronic environment along with steric bulk from the extended side chain of lysine. These changes affect the ATP binding and are reflected by its higher Michaelis-Menton constant for ATP (235.2 ± 15.6 μM) compared to wild-type (4.5 ± 1.1 μM). In spite of the E193K mutant ability to synthesis AdoCbl, its weak affinity for AdoCbl would result in the releasing of cofactor into mitochondrial matrix causing cofactor loss by dilution hence the resulting phenotype. The magnitude of ATP binding impairment in S174L, R190C/H and E193K mutants correlate to their impairment in cob(II)alamin binding suggesting the thermodynamics of ATP binding plays a critical role in the shaping of cob(II)alamin pocket. To understand the active site structure in these mutations, efforts to crystallize these mutant proteins in the presence of ATP is in progress.

3.2) Single nucleotide polymorphic variation in MCM causes increased serum B_{12} levels

Genome-wide association studies (GWAS) of deeply sequenced datasets in human Icelandic and Danish populations have revealed single nucleotide polymorphic (SNPs) variation in various proteins associated with serum B_{12} and folate levels.[15,27,16] SNP variations in multiple proteins involved in the cobalamin trafficking were identified and correlated to B_{12} levels in humans. Among the multiple genome-wide significant associations, the R532H mutation in the coding region of the MUT locus was identified to be associated with increased serum B_{12} levels in humans. MUT locus in humans code for a

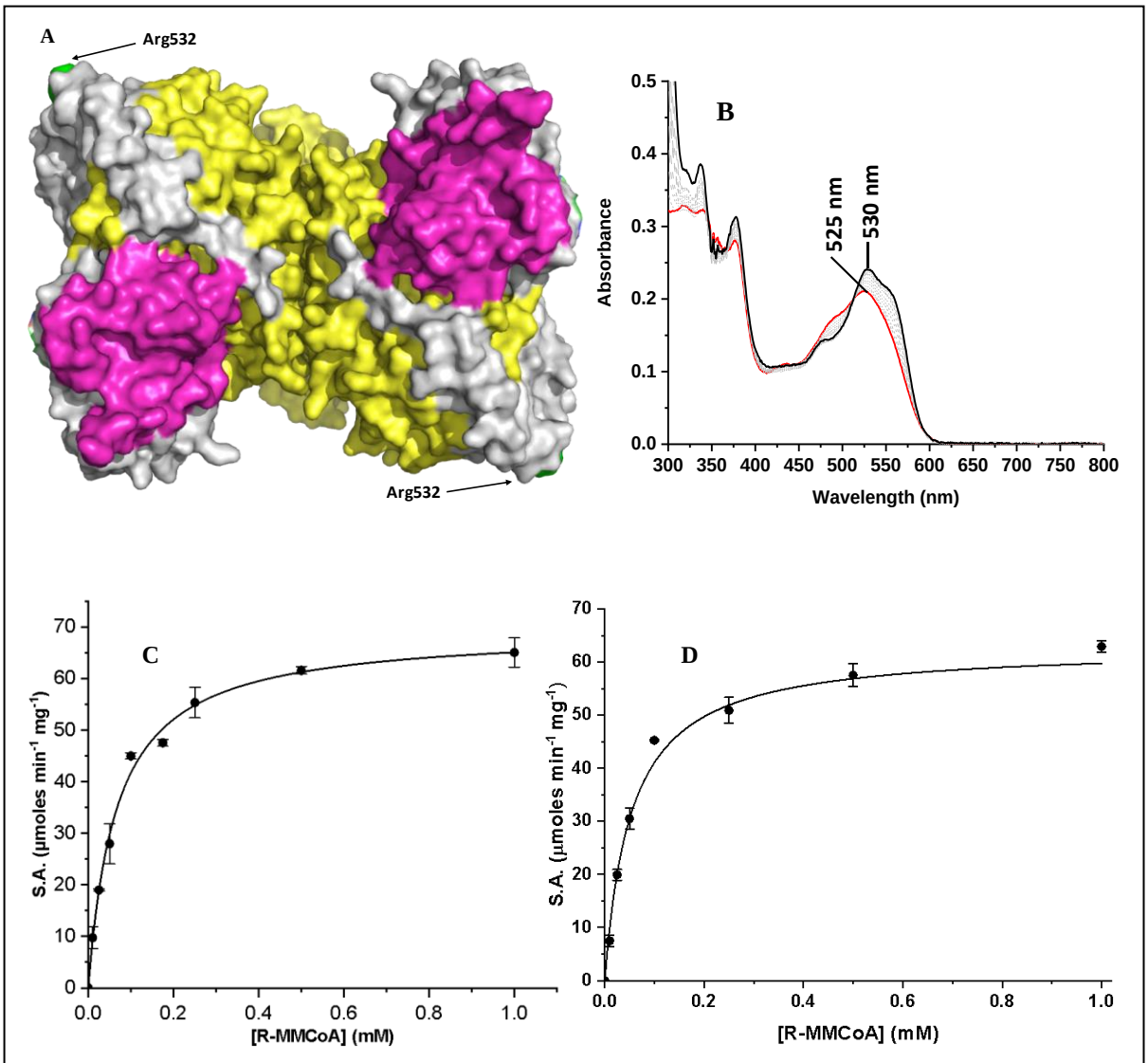

Figure 11: a) structure of MCM homodimer, Arg532 is in an interdomain belt (grey) farther away from the active site. magenta: AdoCbl binding domain, yellow: M-CoA binding domain. b) AdoCbl binding to MCM, red: AdoCbl in solution and black: AdoCbl bound to MCM. c and d) Michaelis-Menten plot of M-CoA turnover activity of wild-type (c) and R532H MCM (d) at variable M-CoA concentrations.

mitochondrial B_{12} utilizing enzyme MCM and the SNP variation on MCM is structurally located in an interdomain belt that connects AdoCbl and M-CoA binding domains and has no direct influence on active site.[14] Expression and stability of R532H (T_m = 51.5 ± 0.3 °C) variant protein was similar to wild-type MCM (T_m = 51.5 ± 0.2 °C).

a. **R532H variation has similar substrate binding like wild-type MCM**

The wild-type MCM and R532H variant protein were analyzed for AdoCbl binding and its turnover activity as mentioned in the methods section. AdoCbl bind MCM in a 'base-off/his-on' six coordinate conformation (λ_{max}= 530 nm) monitored in-vitro by UV-vis spectroscopy. Human MCM exist in homodimer state unlike its bacterial analog and AdoCbl binding titrations were fit to one site per monomer using a dynafit to determine the binding dissociation constant (K_d).[28] Variant R532H bind AdoCbl (K_d = 0.12 ± 0.06 µM) in similar conformation but has a modest increase in affinity compared to wild-type (K_d = 0.27 ± 0.11 µM). Human MCM has a different domain for the AdoCbl and M-CoA binding and the chemistry of isomerization reaction happen in a deeply located active site. Kinetic characterization of M-CoA turnover activity using a coupled S-CoA thiokinase assay indicated R532H variant (V_{max} = 65.2 ± 1.7 µmole min^{-1} mg^{-1}) has a similar catalytic rate like the wild-type MCM (V_{max} = 69.4 ± 1.7 µmole min^{-1} mg^{-1}). The Michaelis-Menten constant indicated R532H mutant (K_m (M-CoA) = 56.0 ± 6.1 µM) also has a similar binding for M-CoA like the wild-type (K_m (M-CoA) = 66.5 ± 6.1 µM).

b. **R532H and wild-type MCM show similar interactions with CblA**

During the catalytic turnover, the adenosyl radical rarely escapes from the active site leading to inactivation by forming a cob(II)alamin bound MCM, the catalytically inactivated cofactor is then transferred on to ATR for the cofactor repair, using energy from the GTP hydrolysis by its G-protein chaperon CblA.[29] CblA uses the GAP activation from MCM for its GTPase activity to transfer the cofactor out of the MCM active site and forms a complex with MCM in the presence of GDP and GTP.[20,30] Analysis of GTPase activity of CblA by HPLC in the presence of R532H variant (K_{act} = 0.5 ± 0.1 µM) indicated similar GAP activation like the wild-type MCM(K_{act} = 0.3 ± 0.1 µM), formation of MCM and CblA complexes were analyzed using size-exclusion chromatography (S200) in the presence of GDP, GMPPCP and GTP (3 min and 20 min incubation). Both MCM (11.9 ml , 174 kDa) and CblA (13.8 ml, 75 kDa) elute with a distinguishable separately on a S200 column, In the presence of 500 µM GDP formation of 2:1 MCM:CblA complex (9.8 ml, 446 kDa) was observed, wherein the presence of nonhydrolyzable GTP analog GMPPCP promoted formation of higher-order oligomers and eluted in void volume (8 ml) of an analytical S200. In the presence of GTP, GAP activation of CblA from MCM results in GTP hydrolysis, hence making it difficult to

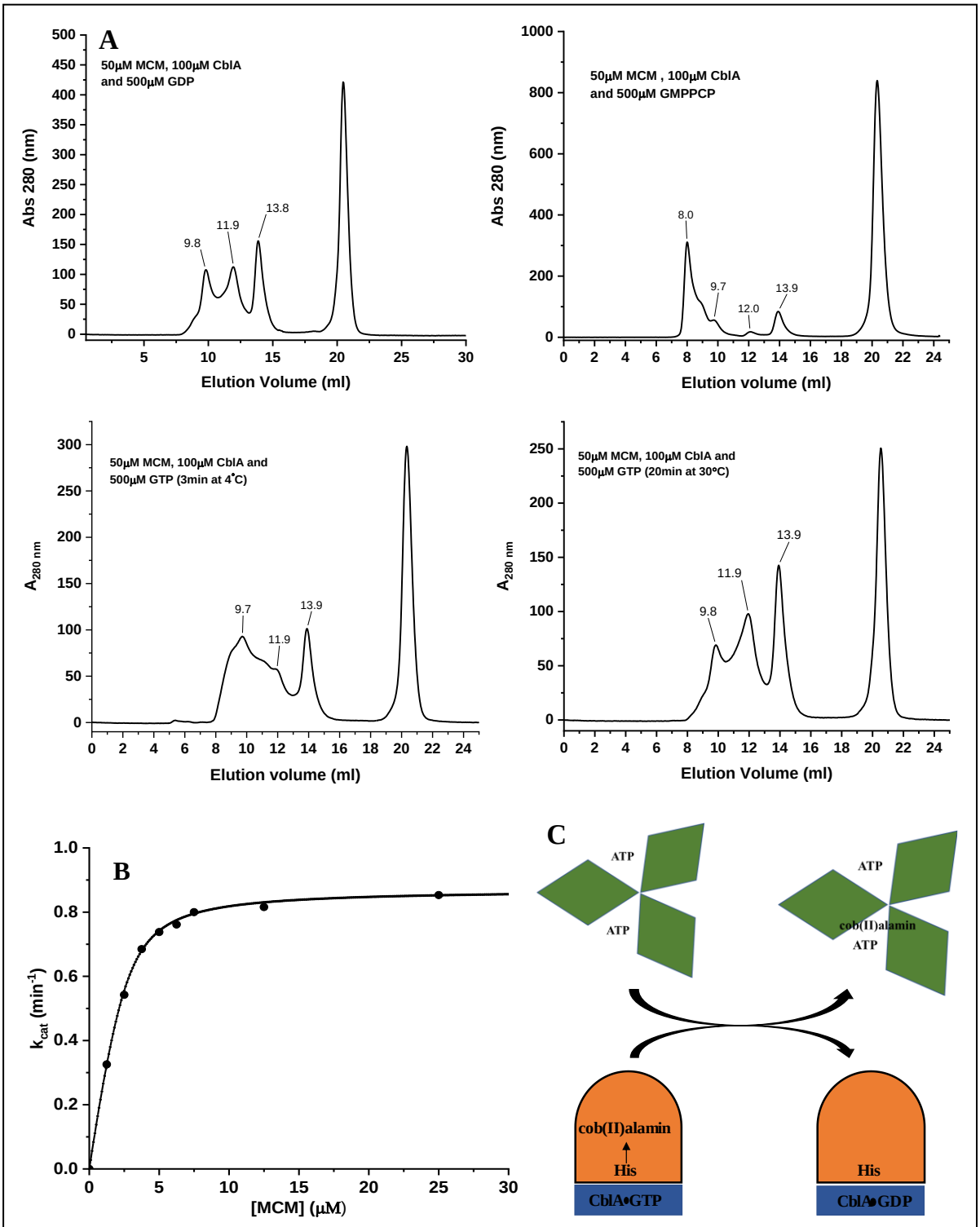

Figure 12: a) MCM and CblA complex formation in the presence of GDP, GMPPCP and GDP b) GTPase activity of 2.5 µM CblA at variable MCM concentrations c) Cob(II)alamin transfer from MCM.CblA complex to ATR.

characterize complex formation in the presence of GTP. Two samples were prepared by incubating with GTP, one for 3 min on ice (to minimize the GTP hydrolysis) and the other incubated for 20 min at 30°C (complete GTP hydrolysis). Elution chromatogram of 3 min sample was similarly close to the elution of MCM and CblA with GMPPCP indicating the the

formation of higher order CblA: MCM oligomeric complexes upon GTP binding, wherein as GTP hydrolyzes (20 min incubation at 30°C) oligomeric complexes fall apart forming 2:1 complex similarly to elution chromatogram observed in the GDP sample. R532H variation didn't perturb the G-nucleotide dependent complex formation of MCM and CblA and was similar to as observed in the wild-type.

c. **AdoCbl transfer from ATR to MCM is slow but complete in R532H MCM**

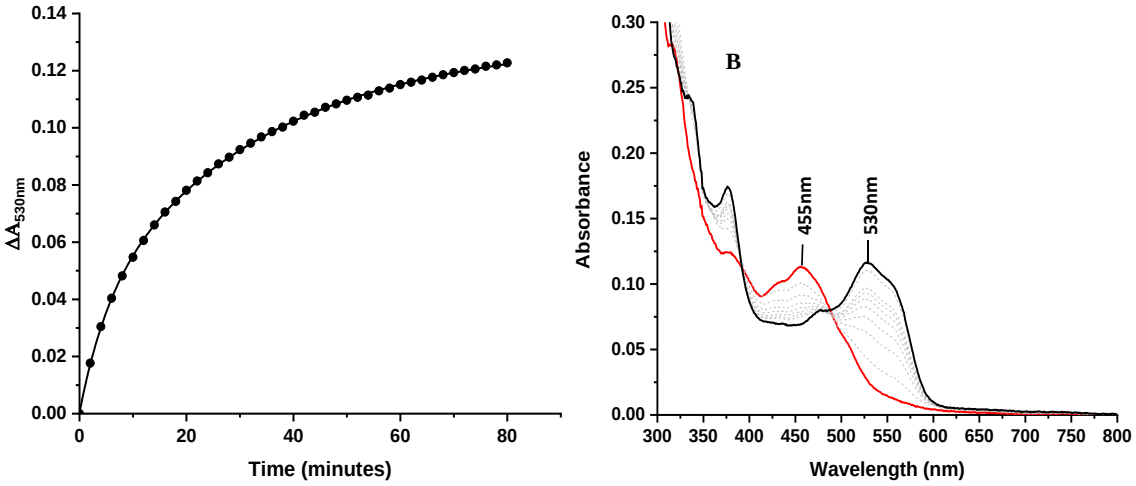

Figure 13: b) AdoCbl transfer from wild-type ATR to R532H MCM, red: AdoCbl bound to ATR and black: AdoCbl bound to R532H MCM a) kinetics of AdoCbl transfer from ATR to MCM measured by change in 530 nm absorbance.

Although the mechanism of cofactor influx into mitochondria still needs to be elucidated, the cofactor entering the mitochondria needs to be transformed into AdoCbl form for the cofactor utilizing enzyme MCM. As discussed in chapter 1, ATR converts the inactive cofactor to active AdoCbl form by an ATP dependent adenosyl transfer reaction. ATR plays an additional role in facilitating the transfer of the synthesized AdoCbl to MCM preventing the cofactor loss into the mitochondrial matrix. The transfer of cofactor from ATR to MCM *in vitro* could be monitored by a UV-vis spectroscopy observing a large red-shift as the AdoCbl changes from five-coordinate 'base-off' conformation (λ_{max} = 455 nm) in ATR to six-coordinate 'base-off/His-on' conformation (λ_{max} = 530 nm) in MCM. The kinetics of AdoCbl transfer from ATR to MCM monitored by the change in absorbance at 530 nm indicated the rate of AdoCbl transfer is slow in R532H MCM compared to wild-type, but both exhibit complete transfer of cofactor, preventing its retention on ATR or dilution into the matrix. Although it is known that ATR and MCM facilitate the transfer of cofactor forms (cob(II)alalmin and AdoCbl) by protein-protein interactions in the mitochondria, structural aspects of ATR and MCM complex formation is still needed to elucidated to understand the effects slow kinetics of AdoCbl transfer reaction.

Kinetic parameter	Wild-type MCM	R532H MCM
k_1	$0.70 \pm 0.01\ min^{-1}$	$0.19 \pm 0.01\ min^{-1}$
k_2	$0.06 \pm 0.01\ min^{-1}$	$0.03 \pm 0.01\ min^{-1}$
A_1	$0.03 \pm 0.01\ min^{-1}$	$0.04 \pm 0.01\ min^{-1}$
A_2	$0.08 \pm 0.01\ min^{-1}$	$0.09 \pm 0.01\ min^{-1}$

Table 4: Kinetic parameters of AdoCbl transfer from ATR to wild-type and R532H MCM.

d. **Conclusion and Future perspectives**

The nonsynonymous mutation in the coding sequences results in a change in the amino acid sequence of functional proteins, these proteins are often further subjected to natural selection resulting in evolution. “Proteins have accumulated these mutations through the billions of years one at a time primarily to create what they are today” (Frances Arnold, *Nobel lecture 2018*). The SNP mutation in MUT locus correlated to high serum B_{12} levels by genomic studies shows a very modest increase in affinity for its substrate M-CoA and AdoCbl compared to wild-type MCM. These changes within the range of experimental error could be physiologically relevant only in the very low abundance of the cofactor in mitochondria. R532H mutation shows no alteration of functions relating to GAP function or its complex formation with CblA in the presence of nucleotides. The physiological effect of a decrease in the rate of AdoCbl transfer from ATR to MCM is less understood as the formation of ATR: MCM complex formation still needs to be elucidated. Genome-wide expression QLT (eQLT) data mapped the MUT sequence variants on its expression and correlated R532H variant to have the strongest effect on MUT expression compared to other variants identified in the non-coding MUT locus.[15] R532H mutations correlation to MUT expression likely to have a larger effect, affecting fatty-acid and branched chain amino acid metabolism as a result of intracellular levels of MCM. We believe that further understanding of cobalamin trafficking including cofactor transport between mitochondria and cytoplasm and ATR complex formation with MCM would help us understand the biochemical functional variation associated with R532H SNP.

REFERENCES:

1 C. Gherasim, M. Lofgren and R. Banerjee, *J. Biol. Chem.*, 2013, **288**, 13186–13193.

2 F. Kalousek, M. D. Darigo and L. E. Rosenberg, *J. Biol. Chem.*, 1980, **255**, 60–5.

3 D. S. Froese, G. Kochan, J. R. C. Muniz, X. Wu, C. Gileadi, E. Ugochukwu, E. Krysztofinska, R. A. Gravel, U. Oppermann and W. W. Yue, *J. Biol. Chem.*, 2010, **285**, 38204–38213.

4 R. Banerjee, *Chem. Rev.*, 2003, **103**, 2083–2094.

5 F. D. Ledley, M. R. Lumetta, H. Y. Zoghbi, P. Vantuinen, S. A. Ledbetter and D. H. Ledbettert, *Mapping of Human Methylmalonyl CoA Mutase (MUT) Locus on Chromosome 6*, 1988, vol. 42.

6 C. Luschinsky Drennan, R. G. Matthews, D. S. ROSENBLATTt, F. D. LEDLEYt, W. A. Fenton, M. L. Ludwig and L. E. Rosenberg, *Molecular basis for dysfunction of some mutant forms of methylmalonyl-CoA mutase: Deductions from the structure of methionine synthase Communicated by*, 1996, vol. 93.

7 L. Tang, H. Deng, X. Zhao and X. Zhang, in *CICTP 2018: Intelligence, Connectivity, and Mobility - Proceedings of the 18th COTA International Conference of Transportation Professionals*, 2018, vol. 106, pp. 1013–1022.

8 M. Yamanishi, M. Vlasie and R. Banerjee, *Trends Biochem. Sci.*, 2005, **30**, 304–308.

9 W. A. Fenton and L. E. Rosenberg, *THE DEFECT IN THE cbl B CLASS OF HUMAN METHYLMALONIC ACIDEMIA:-DEFICIENCY OF COB(I)ALAMIN ADENOSYLTRANSFERASE ACTIVITY IN EXTRACTS OF CULTURED FIBROBLASTS*, vol. 98.

10 E. Vitols, G. A. Walker, ~ And and F. M. Huennekens, *Enzymatic Conversion of Vitamin BIZs to a Cobamide Coenzyme, 45,6=Dimethylbenzimidazolyl)deoxy-adenosylcobamide (Adenosyl-B,)* *, 1966, vol. 241.

11 D. Padovani, T. Labunska, B. A. Palfey, D. P. Ballou and R. Banerjee, *Nat. Chem. Biol.*, 2008, **4**, 194–196.

12 G. C. Campanello, M. Ruetz, G. J. Dodge, H. Gouda, A. Gupta, U. T. Twahir, M. M. Killian, D. Watkins, D. S. Rosenblatt, T. C. Brunold, K. Warncke, J. L. Smith and R. Banerjee, *J. Am. Chem. Soc.*, , DOI:10.1021/jacs.8b08659.

13 J. P. Lerner-Ellis, A. B. Gradinger, D. Watkins, J. C. Tirone, A. Villeneuve, C. M.

Dobson, A. Montpetit, P. Lepage, R. A. Gravel and D. S. Rosenblatt, *Mol. Genet. Metab.*, 2006, **87**, 219–225.

14 D. Sean Froese, G. Kochan, J. R. C Muniz, X. Wu, C. Gileadi, E. Ugochukwu, E. Krysztofinska, R. A. Gravel, U. Oppermann and W. W. Yue, , DOI:10.1074/jbc.M110.177717.

15 N. Grarup, P. Sulem, C. H. Sandholt, G. Thorleifsson, T. S. Ahluwalia, V. Steinthorsdottir, H. Bjarnason, D. F. Gudbjartsson, O. T. Magnusson, T. Sparsø, A. Albrechtsen, A. Kong, G. Masson, G. Tian, H. Cao, C. Nie, K. Kristiansen, L. L. Husemoen, B. Thuesen, Y. Li, R. Nielsen, A. Linneberg, I. Olafsson, G. I. Eyjolfsson, T. Jørgensen, J. Wang, T. Hansen, U. Thorsteinsdottir, K. Stefánsson and O. Pedersen, *PLoS Genet.*, 2013, **9**, 1003530.

16 A. Hazra, P. Kraft, R. Lazarus, C. Chen, S. J. Chanock, P. Jacques, J. Selhub and D. J. Hunter, *Hum. Mol. Genet.*, 2009, **18**, 4677–4687.

17 P. Kuzmič, *Program DYNAFIT for the Analysis of Enzyme Kinetic Data: Application to HIV Proteinase*, 1996, vol. 237.

18 M. Wang, C. Zhu, M. Kohne and K. Warncke, 2015, pp. 59–94.

19 P. W. Riddles, R. L. Blakeley and B. Zerner, *Ellman's Reagent: 5,5'-Dithiobis(2-nitrobenzoic Acid)-a Reexamination*, .

20 D. Padovani and R. Banerjee, , DOI:10.1021/bi0604532.

21 H. L. Schubert and C. P. Hill, *Biochemistry*, 2006, **45**, 15188–15196.

22 T. A. Stich, M. Yamanishi, R. Banerjee and T. C. Brunold, *J. Am. Chem. Soc.*, 2005, **127**, 7660–7661.

23 D. Lexa and J. M. Saveant, *Acc. Chem. Res.*, 1983, **16**, 235–243.

24 W. Bayston, J. H. Bayston, F. D. Looney, J. R. Pilbrow and " E Winfield, *Electron Paramagnetic Resonance Studies of Cob(II)alamin and Cob(II)inamides**, .

25 M. Yamanishi, T. Labunska and R. Banerjee, *J. Am. Chem. Soc.*, 2005, **127**, 526–527.

26 R. Padmakumar, S. Taoka, R. Padmakumar and R. Baneijee, *Coenzyme Bn Is Coordinated by Histidine and Not Dimethylbenzimidazole on Methylmalonyl-CoA Mutase*, 1995, vol. 117.

27 G. Paré, D. I. Chasman, A. N. Parker, R. R. Y. Zee, A. Mälarstig, U. Seedorf, R.

Collins, H. Watkins, A. Hamsten, J. P. Miletich and P. M. Ridker, *Circ. Cardiovasc. Genet.*, 2009, **2**, 142–150.

28 F. Mancia and P. R. Evans, *Conformational changes on substrate binding to methylmalonyl CoA mutase and new insights into the free radical mechanism*, .

29 D. Padovani and R. Banerjee, *Proc. Natl. Acad. Sci.*, 2009, **106**, 21567–21572.

30 N. Korotkova and M. E. Lidstrom, , DOI:10.1074/jbc.M312852200.